International Journal of Thermal Sciences 188 (2023) 108222

Contents lists available at ScienceDirect

International Journal of Thermal Sciences

journal homepage: www.elsevier.com/locate/ijts

Stabilization of levitating clusters containing saltwater droplets

Alexander A. Fedorets [a], Dmitry N. Medvedev [a], Vladimir Yu. Levashov [b], Leonid A. Dombrovsky [a,c,*]

[a] University of Tyumen, 6 Volodarskogo St, Tyumen, 625003, Russia
[b] Moscow State University, 1 Michurinsky Ave., Moscow, 119192, Russia
[c] Joint Institute for High Temperatures, 17A Krasnokazarmennaya St, Moscow, 111116, Russia

ARTICLE INFO

Keywords:
Droplet cluster
Levitation
Saltwater
Evaporation
Condensation
Infrared stabilization

ABSTRACT

The influence of salt (NaCl) dissolved in water on the behavior of levitating droplet clusters, including the formation of equilibrium clusters from saline water droplets during their infrared irradiation, is of interest for further laboratory studies of biochemical processes in individual droplets. Experimental results are presented which show for the first time that even a small salt concentration significantly affects the condensational growth of droplets and their equilibrium size, which is achieved only when the salt concentration is below a certain threshold value. The dependence of this concentration threshold on the surface temperature of the pure water layer under the levitating cluster has been determined. Calculations showed that a correct theoretical description of the evaporation of salt droplets during infrared heating should take into account the asymmetry of the problem related to non-uniform volumetric absorption of radiation and a higher salt concentration at the upper surface of the droplet. The proposed approximate model that takes into account the kinetics of water evaporation and salt diffusion appears to be insufficient to agree well with experimental data. The authors believe that a possible physical reason for the additional decrease in the intensity of evaporation from the upper surface of the droplet is the partial crystallization of salt near the droplet surface due to external infrared irradiation.

1. Introduction

It is known that chemical reactions are accelerated when reactants are present in microdroplets. The reaction rate increases by orders of magnitude with decreasing droplet size. This interesting phenomenon has long attracted the attention of researchers but remains insufficiently studied [1–4]. Laboratory studies require obtaining steadily levitating small water droplets of a given constant size and temperature with dissolved substances contained in the droplets.

Such droplets levitating in an ascending flow of humid air over a locally heated water surface form the so-called droplet cluster [5–8]. A normal droplet cluster is a self-ordered hexagonal structure containing many single droplets. Local heating of the water layer is the main condition for the formation of a droplet cluster [8]. In this case, water evaporates intensively and an upward flow of humid air is produced. Because the room temperature is much lower than the humid air temperature at the water surface and the air contains dust particles, water vapor condenses on these particles and small water droplets are formed. The smallest droplets are carried away by the gas flow, while other droplets have time to increase in size due to condensation of supersaturated vapor and descend by gravity, approaching the water surface. The droplets cannot escape the flow of humid air because the pressure of the surrounding air is noticeably higher. Moreover, the falling water droplets collect in the central zone of the flow, where the gas velocity is higher and the pressure is lower, forming the basis of a cluster. The larger droplets in the central part of the droplet cloud are responsible for the local increase in the gas velocity around them, so droplets located at a greater distance from the vertical axis tend not only to remain in the same plane as the larger droplets but also to be as close to them as possible. Thus, the cloud of droplets is transformed into a flat cluster. The distance between the droplets is determined by the gas flow rate. It is interesting to note that the hexagonal structure of ordinary clusters is changed to a chain structure at a high intensity of evaporation. The physical nature of this reversible transformation is discussed in Ref. [9].

The ordered hexagonal droplet cluster grows both due to the joining of peripheral small droplets and due to vapor condensation, which leads to an increase in the size of droplets. There comes a moment when the most massive droplets coalesce with the water layer and disappear. This limits the cluster lifetime to a few tens of seconds. However, for

* Corresponding author. Joint Institute for High Temperatures, 17A Krasnokazarmennaya St, Moscow, 111116, Russia.
E-mail addresses: ldombr@yandex.ru, ldombr4887@gmail.com (L.A. Dombrovsky).

https://doi.org/10.1016/j.ijthermalsci.2023.108222
Received 17 November 2022; Received in revised form 29 January 2023; Accepted 8 February 2023

Nomenclature

a	droplet radius
c	heat capacity
D	diffusivity
f	coefficient in evaporation model
h	heat transfer coefficient
M	molar mass
$\dot{m}$	mass rate of evaporation
n	index of refraction
Nu	Nusselt number
p	pressure
Q_a	efficiency factor of absorption
q_{rad}	integral radiative flux
R	gas constant
s	mass concentration of salt in water
T	temperature
t	current time
x	diffraction parameter

Greek symbols

α	absorption coefficient
δ	thickness of surface layer
κ	index of absorption
λ	wavelength of radiation
ξ	relative mole fraction
ρ	density
τ	optical thickness
φ	relative humidity

Subscripts and superscripts

air	air
av	average
diff	diffusion
e	external
eq	equilibrium
ev	evaporation
gas	gas
K	Knudsen
max	maximum
mix	mixture
salt	salt
sat	saturation
surf	water surface
t	total
w	water
λ	spectral
0	initial value
*	threshold value

example, external infrared irradiation can completely suppress condensation growth and then the cluster lifetime is limited by the period of maintaining the right conditions [10–12].

In the present study, we use a new technology recently developed in the Laboratory of Microhydrodynamic Technology at the University of Tyumen (Russia). This technology, described below, is based on the use of independently generated small droplets delivered to an area above a heated water layer, where these droplets form a levitating cluster and grow due to condensation of water vapor from an upward flow of humid air. The obvious advantage of such a more flexible procedure compared to the spontaneous formation of a droplet cluster over the heated water surface is that it is possible to work with a droplet cluster and a layer of water of different chemical compositions. This possibility was used by the authors in Ref. [13] to study the first observed self-stabilization of a cluster of pure water droplets levitating over a layer of water containing a small amount of salt. In particular, we were able to determine experimentally the minimum salt concentration at which the equilibrium cluster is formed. Moreover, an analytical model of salt diffusion in the water layer was developed, which gives the correct values of this threshold salt concentration for different surface temperatures of the water layer.

Here we should mention well-known studies of acoustic levitation of droplets [14–16]. The resulting isolated droplets can also be used to study some chemical and biochemical processes. At the same time, it should be noted that it is difficult to obtain spherical droplets that are not subject to shape change in the acoustic wave field. In addition (and this is a significant disadvantage of acoustic levitation) the size of levitating droplets decreases rapidly with evaporation, which does not allow long-term experiments with droplets of constant size. In contrast, the droplet clusters considered in the present paper, levitating over a liquid layer in an ascending flow of humid air, can be stabilized by obtaining steadily levitating equilibrium droplets of constant size.

In the present study, we consider clusters of saltwater droplets levitating over a layer of pure water. The use of salt water brings us closer to the practically important case where the droplets contain water-soluble but not evaporating biological substances. In this case, to obtain an equilibrium cluster, it is necessary to use external infrared radiation, which additionally heats the droplets and increases their evaporation, compensating for the condensation growth of the droplets. Such a method suggested in Refs. [10,11] was successfully used in Ref. [12] to obtain stable equilibrium clusters of pure water droplets. New experiments have shown that salt dissolved in droplets significantly affects the conditions for obtaining equilibrium clusters. The experimental study and physical understanding of this phenomenon is an objective of the present study.

It should be noted that the formation and structure of droplet clusters have attracted the attention of other research groups. In particular, we can mention the works [17–21], which consider various possible mechanisms of cluster formation and the use of droplet clusters to solve some applied problems. However, obtaining equilibrium clusters was not of interest to the applications considered by these authors.

The authors consider the possible use of stable clusters containing droplets with various chemical additives or biological inclusions in studies of the spreading of pollutants or pathogens in the atmosphere. Note that a recent paper [22] considered the possibility of using isolated droplet clusters to study processes associated with viral infections. Of course, viral particles are too small to be directly observed in droplets, but the transformation of certain organic particles or cells by viruses attacking these particles inside the droplets can be studied. Such studies could be useful for understanding the survival conditions of viruses in microdroplets, which spread easily in the atmosphere.

2. Experimental study

2.1. Experimental procedure

The same experimental setup was used as in the experiments [13] on the self-stabilization of a droplet cluster over a layer of salt water. In the selected mode, the piezoelectric dispenser (MicroFab Technologies, Inc., USA) generated three jets of droplets of different sizes (Fig. 1). The droplet size in the stabilized cluster is independent of the initial droplet size, but different amounts of salt in the generated droplets of different sizes (from different jets) allowed for experiments for three different salt concentrations in the equilibrium droplets using the same initial

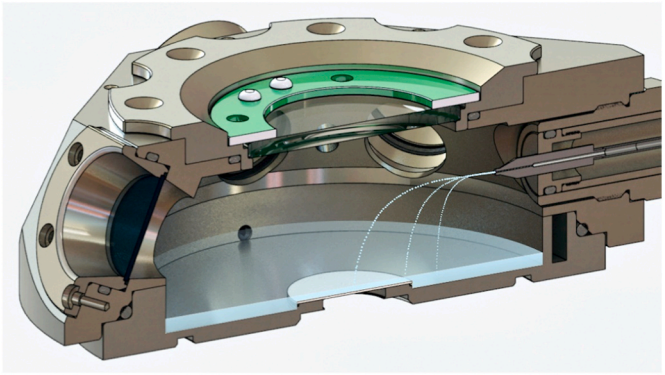

Fig. 1. Working volume of the laboratory setup with microdroplet jets from the dispenser.

solution. Bringing the dispenser nozzle closer to the center of the cuvette reduces the initial size of the cluster droplets. Note that the flow rate of humid air ascending from the locally heated water layer under the cluster is high enough to remove spontaneously condensed microdroplets. As a result, the cluster consists of initially injected droplets throughout the experiment. The cluster was generated over a layer of pure water with an admixture of a surfactant (sodium lauryl sulfate, 0.02 g/l), which is necessary to suppress thermocapillary flow in the water layer [23].

The information on the equipment from a recent paper [13] with minor corrections is briefly reproduced below. The cryothermostat Piccolo 280 OLE (Huber, Germany) allows stabilizing the temperature of the water layer in the metal cuvette. A sitall substrate is glued to the cuvette bottom. The water layer is heated by a laser beam (MRL–III–660D-1W, manufacturer – CNI, China) aimed at the lower blackened surface of the substrate. The thickness of the water layer was controlled by a laser confocal sensor IFC2451 (Micro-Epsilon, USA). The water surface temperature under the cluster was monitored with a CTL-CF1-C3 pyrometric sensor (Micro-Epsilon, USA).

Video recording of the cluster image was carried out using an AXIO Zoom. V16 stereomicroscope (Zeiss, Germany) equipped with a camera Andor iXon Ultra 888 (Oxford Instruments plc, UK). Two video recordings were made in each experiment. The first one covered the moment of droplet injection and the initial 220 s of the cluster life, which allowed, in particular, to measure the initial radius a_0 of the droplets and the unchanged mass of salt in the droplet. The second video recording was made approximately 500 s after the droplet injection. The radius a_{eq} of the equilibrium droplets (average of all droplets in the cluster) was measured from this video recording.

Four miniature EK-8520 infrared sources (Helioworks, USA) without focusing optics were used to stabilize the cluster. The radiation sources were placed symmetrically relative to the vertical axis of the cluster, at an angle of 23° to the horizontal plane at a distance of 42 mm along their axes passing through the droplet cluster. As a result, the cluster and the water layer below it were irradiated almost uniformly. The experiments were performed at a fixed power of infrared sources (supply voltage 3.00 ± 0.01 V). We used the maximum-power radiation mode to stabilize the droplet cluster over the widest range of salt concentrations in the droplets and the surface temperature of the water layer under the cluster. The radiative flux from the infrared sources to every droplet is equal to $q_{rad} = 11.2$ kW/m^2.

The experiments were conducted at three different laser heating powers of the water layer, when the water surface temperature under the cluster was $T_{surf} = 60 \pm 1\ ^\circ C$, $65 \pm 1\ ^\circ C$, and $70 \pm 1\ ^\circ C$. At the same time, the temperature at the periphery of the water layer was maintained at $10 \pm 1\ ^\circ C$. For each of the mentioned thermal regimes, the initial mass concentration of salt in the water varied from $s_0 = 0$ (pure water) in steps of $\Delta s_0 = 0.4$ % to $s_0 = 2$ %. Note that the latter value is more than twice the salt concentration in saline solutions used in medicine and biology [24].

2.2. Experimental results

Typical experimental curves of condensational growth of salt water droplets from the initial radius a_0 to the equilibrium value a_{eq} are shown in Fig. 2a. The concentration of salt in these droplets decreases monotonically from the initial value s_0 to the equilibrium value s_{eq}. Note that droplets with markedly different initial values of radius and salt concentration (variant A, for which $a_0 = 14.6$ μm, $s_0 = 0.8$ % and variant B – $a_0 = 12.9$ μm, $s_0 = 1.2$ %) turn into equilibrium droplets with very close values of both a_{eq} and s_{eq}. This is not surprising, since the amount of salt in the initially larger droplets of cluster A is only 3.4% higher than in the droplets of cluster B.

Fig. 2 shows the parameters of all droplets of clusters A and B. According to Fig. 2a, at each moment of time, the sizes of the droplets of each cluster are practically the same. In this connection, it is interesting to refer to Fig. 3, which gives images of droplet clusters at different moments in time. At the beginning of the process (at $t = 0$) the cluster is still forming, but this process takes less than 5 s, after which the cluster droplets only increase in size.

Note that cluster stabilization, understood as the establishment of equilibrium droplet size with equilibrium salt concentration, does not depend on the number of droplets in the cluster (cluster A has only 10 droplets and cluster B has 12 droplets). This observation is an indirect confirmation of the validity of one of the basic assumptions of the physical model considered below, constructed for a solitary droplet.

Fig. 4 shows the dependences of the equilibrium droplet radius a_{eq} on the mass concentration of salt s dissolved in the droplet for three values of temperature T_{surf} (solid curves with circular symbols). The same figure shows experimental points for the maximum droplet radius at high salt concentration when the infrared irradiation used is insufficient and the droplets coalesce with a layer of water (triangular symbols). As one might expect, the values of a_{max} do not depend on salt concentration because the density of water droplets is almost the same at every $s \leq 0.6$. Points of intersection of curves $a_{eq}(s)$ with horizontal lines $a = a_{max}$ at each of considered values of T_{surf} give maximum values of salt concentration s_{max} at which the used infrared irradiation of the cluster allows to obtain an equilibrium cluster. The experimental data presented in Fig. 4 show that the value of s_{max} decreases with increasing temperature T_{surf}.

The region of infrared stabilization of clusters from saline water droplets under laboratory experiments is presented more clearly in Fig. 5, for the plotting of which all reported data on equilibrium clusters were used. Fig. 5 demonstrates that the threshold concentration of salt in the droplet, s_*, exceeding which in the experimental conditions does not allow to obtain a cluster of equilibrium droplets, monotonically and significantly decreases with increasing temperature of the water layer surface under the cluster.

3. Theoretical modeling

It seems obvious that the physical model of infrared stabilization of small clusters of saline water droplets can rely on the assumption of independent behavior of cluster droplets and refer to any single cluster droplet. Indeed, the experimental results show that the droplets of the considered clusters are almost identical and the number of droplets in the cluster does not affect the equilibrium parameters of single clusters (compare clusters A and B). This assumption also agrees with the theory of radiation scattering by groups of particles [25,26] because the hypothesis of independent scattering of radiation (in physical optics, scattering means both the scattering of radiation itself and the radiation absorption) is valid for droplets whose size and distance between neighboring droplets significantly exceed the wavelength of radiation. It is also obvious that droplets may be considered perfectly spherical. This

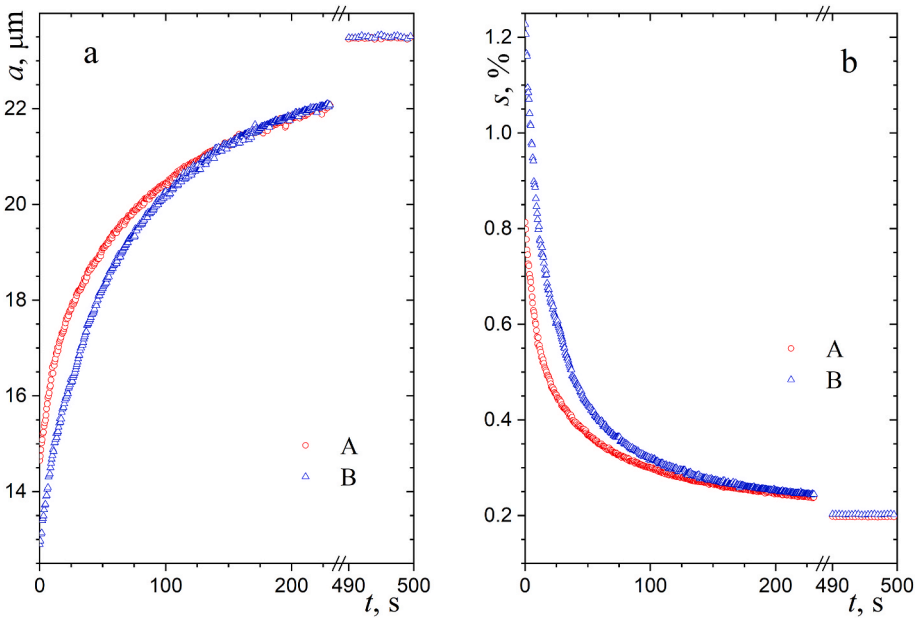

Fig. 2. (a) The condensational growth of droplets and (b) the decrease in the concentration of salt in the droplets in the process of equilibrium cluster formation at $T_{surf} = 65$ °C: A – $a_0 = 14.6$ μm, $s_0 = 0.8$ %, B – $a_0 = 12.9$ μm, $s_0 = 1.2$ %.

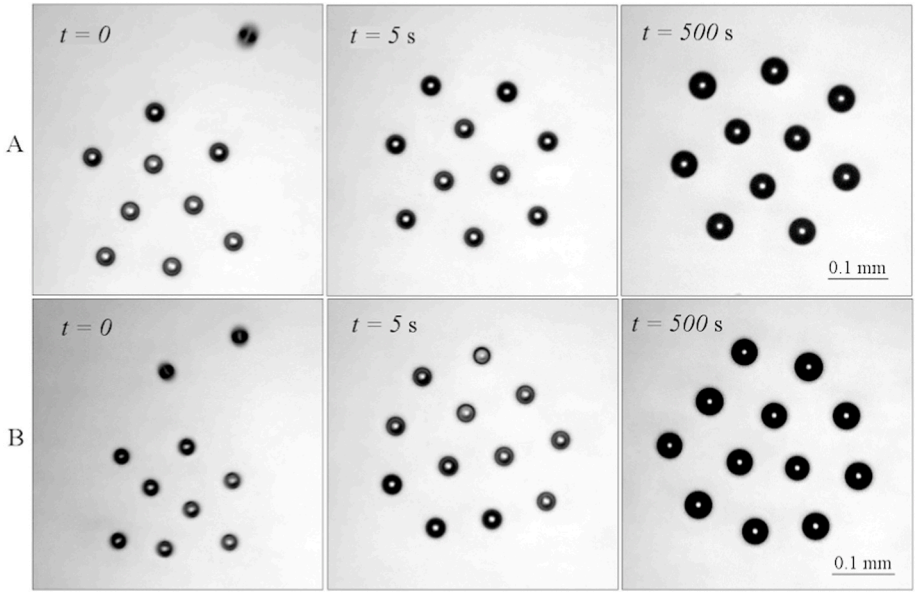

Fig. 3. Images of clusters A and B (see caption to Fig. 2) at different moments of time.

means, in particular, that the calculation of infrared radiation absorption of a droplet can be performed using the classical Mie theory [27–29]. At the same time, the model of isothermal droplets with centrally symmetric evaporation/condensation adopted in Ref. [12] for droplet clusters of pure water droplets may be unacceptable due to dissolved salt and more intense infrared heating of the droplet upper surface by radiation sources located above the cluster. The applicability of the centrally symmetric model of processes in the droplet is discussed below.

3.1. Infrared heating of droplets

For calculations of the absorption of external radiation by an optically homogeneous spherical droplet using the Mie solution, three dimensionless parameters are necessary: the diffraction parameter $x = 2\pi a/\lambda$ of the droplet, the index of refraction n, and the index of absorption κ of the droplet substance. The assumption of optical homogeneity of a droplet containing a salt solution with mass concentration $s < 2$ %, which may be non-uniform over the volume of the droplet, is based on the extremely weak influence of a small amount of dissolved salt on the spectral dependences $n(\lambda)$ and $\kappa(\lambda)$ in the part of the infrared range of interest. The latter statement is confirmed by comparing the experimental data [30] for pure water and similar data [31] for aqueous NaCl solution (see Fig. 6).

According to Mie theory, the absorption of radiation in the volume of a droplet with radius a is characterized by the dimensionless absorption efficiency factor Q_a, which is the ratio of the absorbed radiative flux to the radiative flux per cross-sectional area πa^2 of the droplet. Thus, the integral (over the spectrum) power of infrared radiation absorbed by the droplet is determined as follows:

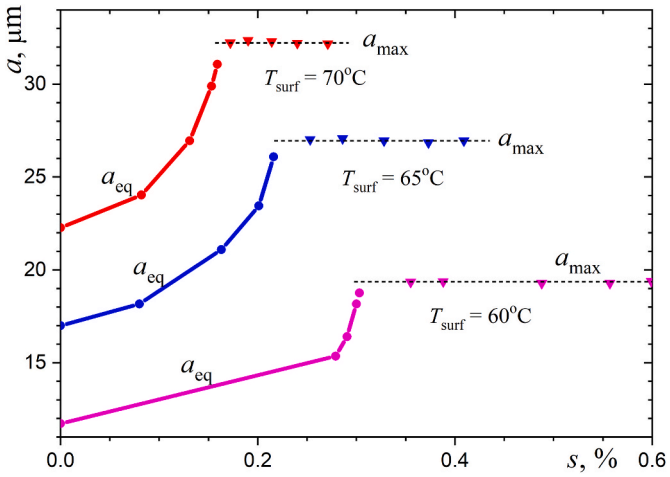

Fig. 4. Equilibrium radii of droplets a_{eq} with salt concentration s and the maximum achievable droplet radius a_{max} before the coalescence with a layer of pure water: experimental data for three values of water surface temperature T_{surf}.

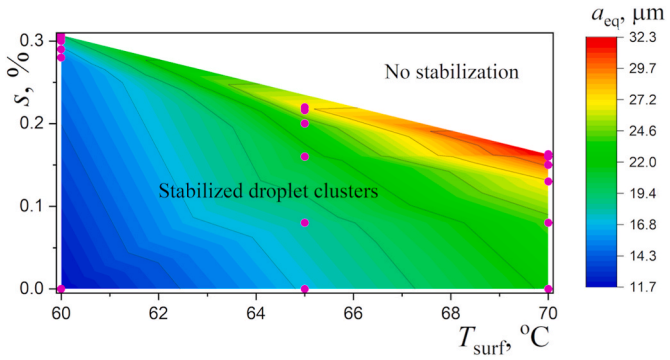

Fig. 5. The region of stabilized clusters of saltwater droplets. Violet circles are some of the points from Fig. 4.

$$P(a) = \overline{Q}_a(a) \times \pi a^2 q_{rad}, \quad \overline{Q}_a(a) = \int_{\lambda_1}^{\lambda_2} Q_a(\lambda, a) I_b(\lambda, T_e) d\lambda \Big/ \int_{\lambda_1}^{\lambda_2} I_b(\lambda, T_e) d\lambda, \tag{1}$$

where $\overline{Q}_a$ is the average efficiency factor of absorption, $I_b(\lambda, T_e)$ is the Planck function for the blackbody radiation of the emitters at temperature $T_e = 1223$ K, and a choice of λ_1 and λ_2 is determined by the Planck function and the spectral dependence of the efficiency factor of absorption. Note that the influence of a small reflection of radiation from the water layer under the cluster can also be neglected [12]. The dependence of $\overline{Q}_a(a)$ calculated by Eq. (1) is shown in Fig. 7. In addition to the value of $\overline{Q}_a$, determined, according to Eq. (1), by integration over the whole spectrum, Fig. 7 shows the dependence of $\overline{Q}_a(a)$ obtained without taking into account the absorption of radiation by a droplet in the wavelength range $2.6\,\mu m < \lambda < 3.6\,\mu m$, i.e. in the region of the strongest water absorption band. A comparison of the two curves in Fig. 7 shows a significant contribution of the absorption band: 25% for

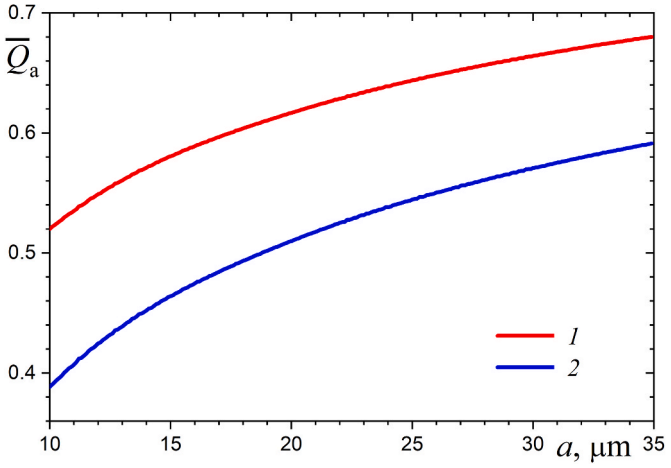

Fig. 7. Averaged over the infrared spectrum efficiency factor of absorption: *1* – for the complete spectrum, *2* – excluding the wavelength range of $2.6\,\mu m < \lambda < 3.6\,\mu m$.

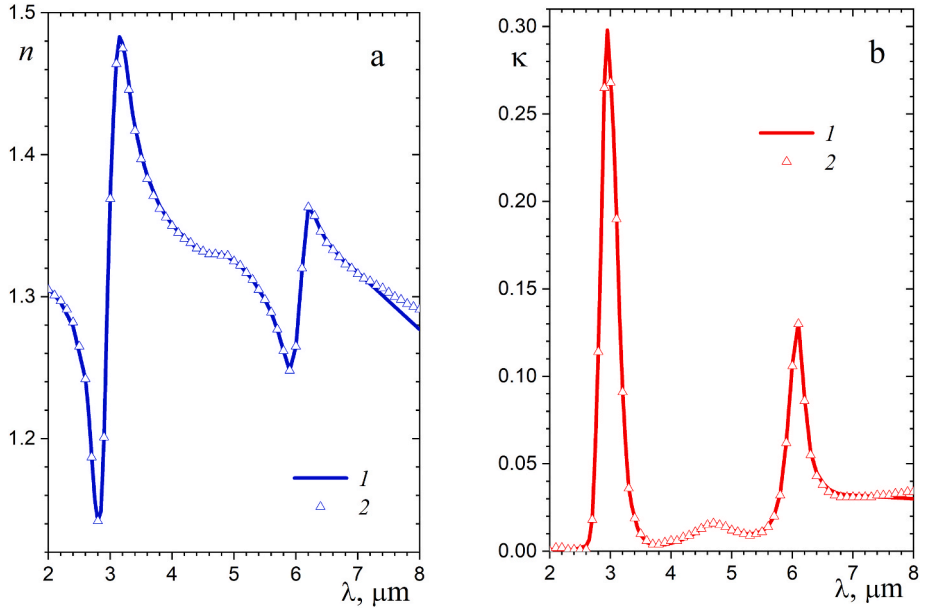

Fig. 6. (a) Index of refraction and (b) index of absorption in the infrared range of external irradiation of a droplet cluster: 1 – $s = 0$ (pure water) [26], 2 – $s = 1.461$ % (saltwater) [27].

droplets of radius a = 10 μm and 14% for droplets of radius 30 μm. Apparently, absorption of radiation by droplets in the water absorption band deserves special attention.

Generally speaking, the infrared radiation is absorbed nonuniformly over the volume of the droplet, and this strongly depends on the spectral interval because of the significant variation of the absorption index (Fig. 6b). For example, at a wavelength $\lambda = 2.4$ μm we have $\kappa = 0.001$ and in the absorption band of water, at $\lambda = 3$ μm, we have $\kappa \approx 0.3$. Both of these wavelengths are close to the maximum of the Planck function at temperature $T_e = 1223$ K (according to Wien's displacement law, the point of the maximum is at wavelength $\lambda = 2.37$ μm). Therefore, the blackbody radiation intensity at $\lambda = 3$ μm in only 12% less than at $\lambda = 2.4$ μm.

At $\kappa = 0.001$ water absorption coefficient $\alpha_\lambda = 4\pi\kappa/\lambda = 5.3 \times 10^3$ m^{-1} and optical thickness of the droplet with radius $a = 20$ μm is equal to $\tau_\lambda = \alpha_\lambda a \approx 0.1$. At such a small optical thickness, the absorption of radiation in a large droplet with diffraction parameter $x = 53$ is very small (most of the radiation passes through the droplet) and, besides, because of refraction, according to the laws of geometrical optics, this absorption occurs far from the illuminated surface [32,33]. On the contrary, at wavelength $\lambda = 3$ μm, where the spectral radiative flux is also large, the optical thickness of the same droplet $\tau_\lambda = 25.1$ and practically all radiation except a small reflected one is absorbed in a thin surface layer of the droplet with thickness $\delta_\lambda = 2/\alpha_\lambda \approx 1.6$ μm. The latter is extremely important because it means that a considerable part of the incident infrared radiation is absorbed in the thin surface layer at the top of the droplet.

For pure water droplets in Ref. [12], the predominant infrared heating of the surface layer in the upper part of the droplet turned out to be less important because the radiative flux is half as large as the thermal effect of absorbed radiation was partially compensated by heat conduction. Therefore, the isothermal droplet model proposed in Ref. [12] described well the experimental data on equilibrium cluster formation. Perhaps, for saltwater droplets, we should pay attention to another result of asymmetric radiative heating: more intense evaporation of water from the upper surface of the droplet increases the local salt concentration, which is maintained at a higher level, preventing further evaporation and thereby weakening the stabilizing role of infrared irradiation. This may be important because of the very small value of the diffusion coefficient of salt in water. For example, $D_{salt} \approx 3\times 10^{-9}$ m^2/s at water temperature 60 °C [34,35]. However, for saltwater droplets with a radius $a < 35$ μm (Fig. 2), the characteristic relaxation time for salt concentration over the droplet volume $t_{diff} = a^2/D_{salt} < 0.5$ s. This means that the radial salt concentration profile can be calculated in the quasi-steady-state approximation.

In connection with the discussion of the role of infrared radiation in the evaporation of droplets, it should be recalled that first-order phase transitions, such as water vapor condensation, are accompanied by characteristic infrared radiation. This so-called PeTa effect may be important for remote sensing of the cloudy atmosphere [36,37]. However, the radiative heat loss in the range of $4\,\mu m < \lambda < 8\,\mu m$ during condensation of water vapor does not exceed 3–5% of the latent energy of the phase transition. Therefore, this effect is neglected in the present study.

3.2. The centrally-symmetric model

The above arguments in favor of an asymmetric temperature field and, most importantly, asymmetric salt concentration field in spherical droplets, including equilibrium cluster droplets, do not exclude consideration of a simple centrally-symmetric model. Note that a similar model proved quite successful for pure water droplets [12].

Following [12] we will assume that temperature in small droplets is uniform due to the significant thermal conductivity of water. It is also assumed that the concentration of salt in the droplets is uniform. As for pure water droplets, the temperature of the droplets, T, and their radius, a, can be determined by solving the Cauchy problem for the coupled first-order ordinary differential equations [12,38]:

$$\rho_w c_w \frac{dT}{dt} = \frac{3}{a}\left(\frac{\overline{Q}_a q_{rad}}{4} + \dot{m}L - k_{air}\frac{T - T_{air}}{a}\right), \quad T(0) = T_0, \tag{2}$$

$$\rho_w \frac{da}{dt} = \dot{m}, \quad a(0) = a_0, \tag{3}$$

where $\rho_w = 10^3$ kg/m^3 and $c_w = 4.18$ kJ/kg are the density and specific heat capacity of water, $\dot{m}$ is the mass rate of the droplet evaporation measured in kg/(m^2 s), $L = 2.26$ MJ/kg is the latent heat of water evaporation, $k_{air} = 0.026$ W/(m K) is the thermal conductivity of air, and T_{air} is the temperature of ambient air. When writing the convective term in Eq. (2) it has been taken into account that in the Stokes flow regime around the sphere the Nusselt number Nu = 2 and therefore the convective heat transfer coefficient is expressed as $h = \mathrm{Nu} \times k_{air}/(2a) = k_{air}/a$.

The value of $\dot{m}$ is determined by the following equation [39,40]:

$$\dot{m} = \frac{D_{vap} p_{air}}{a R_{air}(T_{air}, \varphi_{air}) T_{air}} \ln \frac{1 - \xi_w \psi(T, \varphi_K)\varphi_K}{1 - \psi(T_{air}, \varphi_{air})\varphi_{air}}, \quad \psi(T, \varphi) = \frac{p_{sat}(T)}{p_{air}} \frac{M_{vap}}{M_{air}(T, \varphi)}, \tag{4}$$

and the relative humidity at the Knudsen layer boundary is calculated using the mass balance equation:

$$f_{ev}\xi_w \frac{p_{sat}(T)}{\sqrt{2\pi R_{vap} T}}(\varphi_K - 1) = \frac{D_{vap} p_{air}}{a R_{air}(T_{air}, \varphi_{air}) T_{air}} \ln \frac{1 - \xi_w \psi(T, \varphi_K)\varphi_K}{1 - \psi(T_{air}, \varphi_{air})\varphi_{air}}. \tag{5}$$

where D_{vap} is the diffusion coefficient for water vapor in air, $R_{air} = R/M_{air}$ ($R = 8314$ J/(kmol K) is the universal gas constant) is the gas constant for the humid air, p_{air} is the atmospheric pressure, p_{sat} is the pressure of saturated water vapor, M_{vap} and M_{air} are the molar masses of water vapor and humid air, φ_K and φ_{air} are the values of relative humidity of air at the boundary of Knudsen layer and outside the boundary layer of viscous gas flow, respectively. The molar mass of humid air is calculated as:

$$M_{air}(T, \varphi) = M_{air,0} - \varphi\left(M_{air,0} - M_{vap}\right)\frac{p_{sat}(T)}{p_{air}}, \tag{6}$$

where $M_{vap} = 18$ and $M_{air,0} = 29$ is the molar mass of dry air.

Equations (4) and (5) are only slightly modified compared to the corresponding equations for the droplet of pure water [12,38] by introducing the local mole fraction of water in salt solution:

$$\xi_w = \frac{1}{1 + \overline{M}_{vs} s/(1 - s)}, \tag{7}$$

where $\overline{M}_{vs} = M_{vap}/M_{salt} = 0.308$. This modification corresponds to Raoult's law for the effect of water salinity. Since $s \ll 1$, the formula for ξ_w can be written as:

$$\xi_w = 1 - \overline{M}_{vs} s. \tag{8}$$

The pressure of the saturated vapor of water is calculated using the Antoine equation with the parameters reported in Ref. [41]:

$$\lg p_{sat}(T) = 9.6543 - 1435.264\,/\,(T - 64.848), \tag{9}$$

where T is measured in Kelvin and p_{sat} is obtained in Pascal. The coefficient $f_{ev} = 0.0024$ in Eq. (5) was introduced in Refs. [40,42] for water droplets in air to avoid the complicated numerical solution. The above model agrees well with experimental data of [43].

The balance of evaporation and condensation is written as $\dot{m} = 0$, since this physical quantity is considered as a net mass flow rate due to evaporation and condensation ($\dot{m} > 0$ for the prevailing evaporation). In

this case, the temperature of the equilibrium droplet (when evaporation and condensation of water balance each other), T_{eq} is determined from the balance of heat input by infrared radiation and output from the droplet to the cooler ambient air with temperature T_{air}:

$$P(a_{eq}) = 4\pi a_{eq}^2 \times \mathrm{Nu}\frac{k_{air}}{2a_{eq}}(T_{eq} - T_{air}), \tag{10}$$

where Nu is the Nusselt number, which is equal to 2 for the Stokes flow regime. As in Ref. [12] we assume that $T_{air} = T_{surf}$ because the height of the cluster levitation is very small [44]. The resulting relation for T_{eq} is as follows:

$$T_{eq} = T_{surf} + \frac{a_{eq}}{4k_{air}}\overline{Q}_a(a_{eq})q_{rad}. \tag{11}$$

Note that the value of T_{eq} does not depend on both the salinity of water and the air humidity.

Consider the condition of the droplet equilibrium, which follows from Eqs. (4) and (5) at $\dot{m} = 0$:

$$\xi_w \psi(T, \varphi_K)\varphi_K = \psi(T_{air}, \varphi_{air})\varphi_{air}, \quad \varphi_K = 1. \tag{12}$$

The resulting equation for the threshold value of the salt concentration is as follows:

$$\xi_w(s_*) = \varphi_{air}\psi(T_{air}, \varphi_{air}) \Big/ \psi\left(T_{eq}^{max}, 1\right). \tag{13}$$

To verify the physical model discussed above, calculations were performed for various experimental values of the water surface temperature. As one might expect, the calculations for pure water droplets gave the correct value of the equilibrium radius of the droplets, coinciding with the experimental value. At the same time, the calculations showed a very weak influence of salt on the equilibrium radius of saline water droplets. The computational results for droplets with initial radius $a_0 = 10$ μm over at $T_{surf} = 65$ °C showed an increase in the equilibrium radius from 16.91 μm for pure water droplets to only 17.14 μm for saltwater droplets, which is radically different from the significant increase in the equilibrium radius of saltwater droplets observed in the experiment (see Fig. 4).

3.3. Approximate asymmetric model

The analysis showed that to build a correct model of evaporation of a droplet of salt water heated from above by infrared radiation, a relatively high salt concentration near the droplet's upper surface should be considered. A similar problem was solved in Ref. [13] for a layer of salt water under a cluster. In both cases, the salt concentration drop is provided by salt diffusion directed downward.

Strictly speaking, the salt concentration monotonically decreases along the droplet surface to a minimum value at the lower point of the surface. Nevertheless, in an approximate model, as in a flat layer of salt water, we can assume that the salt concentration s_{max} is constant on the upper surface of the droplet and that the salt concentration is zero on the lower surface of the same area. The latter assumption is acceptable because the low salt concentration does not affect the evaporation rate. The distance between the lower and upper surfaces of the model volume is assumed to be equal to the diameter of the droplet.

The natural assumption of temperature constancy in a small droplet of water (due to the high thermal diffusivity) means that the salt diffusion coefficient can be assumed constant over the volume of the droplet. The calculation of the salt concentration field in a spherical droplet is rather complicated. Therefore, taking into account considerable uncertainty in the variation of heat transfer conditions along the droplet surface it makes sense to limit ourselves to an approximate physical estimate. This estimation is obtained from the solution of the problem for a flat layer of salt water with a thickness equal to the droplet diameter. In the quasi-steady approximation, the salt concentration profile in a flat layer of water can be considered parabolic [13]. Using the mass balance conditions on the lower and upper surfaces of the droplet, one can obtain the following relation for the current value of $s_{max}(t)$:

$$s_{max}\frac{D_{salt}}{2a} = \frac{3\dot{m}(s_{max}) - \dot{m}(0)}{4\rho_w}, \tag{14}$$

where $\dot{m}(s)$ is determined by Eqs. (4) and (5). The doubled factor in the denominator of the right-hand side of equation (14) is due to the fact that the areas of the upper and lower surfaces are half of the total droplet surface for which $\dot{m}(s)$ values are calculated. Equation (3) can still be used to calculate the droplet radius, but instead of the former value $\dot{m}$ determined by the symmetric evaporation model, the new value of the total mass rate of evaporation should be used:

$$\dot{m}_t = \frac{\dot{m}(s_{max}) + \dot{m}(0)}{2}. \tag{15}$$

Calculation of the salt concentration profile in a droplet of water, for example, at $T_{surf} = 65$ °C gives the value $s_{max} = 0.98$ %, which is significantly higher than the average salt concentration in a droplet, which is equal to 0.22%. Nevertheless, as can be seen in Fig. 8, the calculated equilibrium radius increases from $a_{eq} = 16.9$ μm for a droplet from pure water only to $a_{eq} = 17.4$ μm due to dissolved salt. The latter value is significantly less than the experimental value $a_{eq} = 27$ μm. However, the computational model based on the assumption of absence of salt particles suspended in water as well as a salt crust on the upper surface of the droplet shows the physically obvious increase of the equilibrium droplet radius with increasing salt concentration.

One cannot exclude that a possible physical reason for the additional strong decrease in the intensity of evaporation from the upper surface of the droplet is the partial crystallization of salt near the droplet surface. It is known that at a high salt concentration, a gradually compacted solid crust is formed on the droplet surface, preventing water evaporation. This phenomenon, studied in Refs. [45–48], was taken into account by the authors in calculating the heating of seawater droplets in a mist curtain used for shielding the thermal radiation of large fires [38,49].

In the case of convective heating of relatively large water droplets, the formation of salt particles from aqueous solution is usually starts at mass fraction of salt greater than about 26%. In our case, we are dealing with much smaller droplets than those usually considered in drying problems. According to Refs. [1–4], the rate of various kinds of transformations, including crystallization of dissolved matter, is much higher in microdroplets. In addition, in the considered problem, salt water droplets are heated not due to convective heat transfer from warmer air near the droplet surface, but as a result of volumetric absorption of

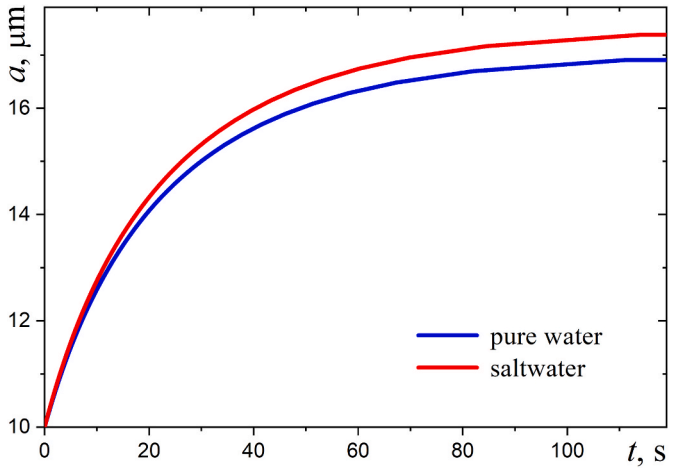

Fig. 8. Calculated time variation of the droplet radius for the infrared irradiation of the droplet cluster levitating over the water layer surface with temperature $T_{surf} = 65$ °C.

infrared radiation in the droplet. Probably, the mentioned circumstances can lead to the formation of small salt crystals already at a salt concentration $s \approx 1$ %. Of course, this question requires further investigation.

4. Conclusions

The effect of salt dissolved in water on the formation of equilibrium droplet clusters was studied experimentally and a theoretical analysis of the experimental results is given. It is expected that the problem considered will be important for further laboratory studies of biochemical processes in the droplets. Experimental results obtained at different temperatures of the substrate water surface showed for the first time that even a small salt concentration significantly affects the condensational growth of droplets and their equilibrium size, which is achieved only when the salt concentration is below a certain threshold value.

Two theoretical models that take into account the influence of dissolved salt on the stabilization of a cluster of saltwater droplets by means of external infrared radiation are considered. As expected, the simplest model, in which the salt concentration was assumed constant over the droplet volume, gives no significant effect of salt on droplet growth dynamics. Calculations have shown that it is necessary to take into account the preferential absorption of infrared radiation in the upper part of the droplet, which leads to more intensive evaporation and increased salt concentration near the illuminated surface of the droplet and this effect is only partially compensated by salt diffusion. These features of the problem were taken into account in the asymmetric model, which gave already a noticeable, but much smaller than observed, increase in the equilibrium size of the saltwater droplets.

In our opinion, the physical reason why the calculation results differ from the experimental data is due to the assumption that the droplet does not contain suspended salt particles and that not even a thin crust of salt forms on its surface. This assumption was based on data for large solution volumes in which solid particles appear at much higher salt concentrations. It is likely that the formation of salt particles in microdroplets occurs at much lower salt concentrations. Of course, this hypothesis needs to be examined in further studies.

Declaration of competing interest

The authors declare that they have no known competing financial interests or personal relationships that could have appeared to influence the work reported in this paper.

Data availability

Data will be made available on request.

Acknowledgments

The authors are grateful for the financial support of this work by the Ministry of Science and Higher Education of the Russian Federation (project no. FEWZ-2023-0002).

References

[1] Z. Wei, Y. Li, R.G. Cooks, X. Yan, Accelerated reaction kinetics in microdroplets: overview and recent developments, Annu. Rev. Phys. Chem. 71 (2020) 31–51, https://doi.org/10.1146/annurev-physchem-121319-110654.

[2] Y. Zhang, M.J. Apsokardu, D.E. Kerecman, M. Achtenhagen, M.V. Johnston, Reaction kinetics of organic aerosol studied by droplet assisted ionization: enhanced reactivity in droplets relative to bulk solution, J. Am. Soc. Mass Spectrom. 32 (1) (2021) 46–54, https://doi.org/10.1021/jasms.0c00057.

[3] Y. Zhang, Mechanisms and Kinetics of Enhanced Reactivity in Droplets Relative to Bulk Solution, PhD Thesis, Univ. Delaware, 2022. https://udspace.udel.edu/handle/19716/30799.

[4] K. Li, K. Gong, J. Liu, L. Ohnoutek, J. Ao, Y. Liu, X. Chen, G. Xu, X. Ruan, H. Cheng, J. Han, G. Sui, M. Ji, V.K. Valev, L. Zhang, Significantly accelerated photochemical and photocatalytic reactions in microdroplets, Cell Rep. Phys. Sci. 3 (6) (2022), 100917, https://doi.org/10.1016/j.xcrp.2022.100917.

[5] A.A. Fedorets, Droplet cluster, JETP Lett. 79 (8) (2004) 372–374, https://doi.org/10.1134/1.1772434.

[6] A.A. Fedorets, M. Frenkel, E. Shulzinger, L.A. Dombrovsky, E. Bormashenko, M. Nosonovsky, Self-assembled levitating clusters of water droplets: pattern-formation and stability, Sci. Rep. 7 (2017) 1888, https://doi.org/10.1038/s41598-017-02166-5.

[7] A.A. Fedorets, E. Bormashenko, L.A. Dombrovsky, M. Nosonovsky, Droplet clusters: nature-inspired biological reactors and aerosols, Philos. Trans. Royal Soc. A 377 (2150) (2019), 20190121, https://doi.org/10.1098/rsta.2019/0121.

[8] A.A. Fedorets, L.A. Dombrovsky, D.V. Shcherbakov, E. Bormashenko, M. Nosonovsky, Thermal conditions for the formation of self-assembled cluster of droplets over the water surface and diversity of levitating droplet clusters, Heat Mass Tran. (2022), https://doi.org/10.1007/s00231-022-03261-8 published online 28 June 2022.

[9] A.A. Fedorets, M. Frenkel, I. Legchenkova, D. Shcherbakov, L. Dombrovsky, M. Nosonovsky, E. Bormashenko, Self-arranged levitating droplet clusters: a reversible transition from hexagonal to chain structure, Langmuir 35 (47) (2019) 15330–15334, https://doi.org/10.1021/acs.langmuir.9b03135.

[10] A.A. Fedorets, L.A. Dombrovsky, D.N. Medvedev, Effect of infrared irradiation on the suppression of the condensation growth of water droplets in a levitating droplet cluster, JETP Lett. 102 (7) (2015) 452–454, https://doi.org/10.1134/S0021364015190042.

[11] L.A. Dombrovsky, A.A. Fedorets, D.N. Medvedev, The use of infrared irradiation to stabilize levitating clusters of water droplets, Infrared Phys. Technol. 75 (2016) 124–132, https://doi.org/10.1016/j.infrared.2015.12.020.

[12] L.A. Dombrovsky, A.A. Fedorets, V.Yu. Levashov, A.P. Kryukov, E. Bormashenko, M. Nosonovsky, Stable cluster of identical water droplets formed under the infrared irradiation: experimental study and theoretical modeling, Int. J. Heat Mass Tran. 161 (2020), 120255, https://doi.org/10.1016/j.ijheatmasstransfer.2020.120255.

[13] A.A. Fedorets, D.V. Shcherbakov, V.Yu. Levashov, L.A. Dombrovsky, Self-stabilization of droplet clusters levitating over heated salt water, Int. J. Therm. Sci. 182 (2022), 107822, https://doi.org/10.1016/j.ijthermalsci.2022.107822.

[14] A.L. Yarin, G. Brenn, O. Kastner, D. Rensink, C. Tropea, Evaporation of acoustically levitating droplets, J. Fluid Mech. 399 (1999) 151–204, https://doi.org/10.1017/S0022112099006266.

[15] D. Zang, Y. Yu, Z. Chen, X. Li, H. Wu, X. Geng, Acoustic levitation of liqud drops: dynamics, manipulation and phase transitions, Adv. Colloid Interface Sci. 243 (2017) 77–85, https://doi.org/10.1016/j.cis.2017.03.003.

[16] Y. Maruyama, K. Hasegawa, Evaporation and drying kinetics of water-NaCl droplets *via* acoustic levitation, RSC Adv. 10 (4) (2020) 1870, https://doi.org/10.1039/c9ra09395h.

[17] A.V. Shavlov, V.A. Dzhumandzhi, S.N. Romanyuk, Electrical properties of water drops inside the dropwise cluster, Phys. Lett. 376 (1) (2011) 39–45, https://doi.org/10.1016/j.physleta.2011.10.032.

[18] A.V. Shavlov, S.N. Romanyuk, V.A. Dzhumandzhi, Effective charge and effective radius of water droplet in dropwise cluster, Phys. Plasmas 20 (2) (2013), 023703, https://doi.org/10.1063/1.4792260.

[19] T. Umeki, M. Ohata, H. Nakanishi, M. Ichikawa, Dynamics of microdroplets over the surface of hot water, Sci. Rep. 5 (2015) 8046, https://doi.org/10.1038/srep08046.

[20] D.V. Zaitsev, P.P. Kirichenko, V.S. Ajaev, O.A. Kabov, Levitation and self-organization of liquid microdroplets over dry heated substrates, Phys. Rev. Lett. 119 (9) (2017), 094503, https://doi.org/10.1103/PhysRev.Lett.119.094503.

[21] D.V. Zaitsev, P.P. Kirichenko, A.I. Shatekova, O.A. Kabov, V.S. Ajaev, Levitation conditions for condensing droplets over heated liquid surfaces, Soft Matter 17 (17) (2021) 4623–4631, https://doi.org/10.1039/d0sm02185g.

[22] L.A. Dombrovsky, A.A. Fedorets, V.Yu. Levashov, A.P. Kryukov, E. Bormashenko, M. Nosonovsky, Modeling evaporation of water droplets as applied to survival of airborne viruses, Atmosphere 11 (9) (2020) 965, https://doi.org/10.3390/atmos11090965.

[23] A.A. Fedorets, D.V. Shcherbakov, L.A. Dombrovsky, E. Bormashenko, M. Nosonovsky, Impact of surfactants on the formation and properties of droplet clusters, Langmuir 36 (37) (2020) 11154–11160, https://doi.org/10.1021/acs.langmuir.0c02241.

[24] M. Savva, Isotonic solutions, in: Pharmaceutical Calculations", Springer Nature Switzerland, Cham, 2019.

[25] M.I. Mishchenko, Electromagnetic Scattering by Particles and Particle Groups: an Introduction, Cambridge University Press, Cambridge (UK), 2014, https://doi.org/10.1017/CBO9781139019064. Online ISBN: 978-1-139019-064.

[26] M.I. Mishchenko, "Independent" and "dependent" scattering by particles in a multi-particle group, OSA Continuum 1 (1) (2018) 243–260, https://doi.org/10.1364/OSAC.1.000243.

[27] H.C. Van de Hulst, Light Scattering by Small Particles, Dover Publ., New York, 1981. ISBN: 978-04866442284.

[28] C.F. Bohren, D.R. Huffman, Absorption and Scattering of Light by Small Particles, Print ISBN: 9780471293408, Wiley, New York, 1998, https://doi.org/10.1002/9783527618156. Online ISBN: 9783527618156.

[29] L.A. Dombrovsky, D. Baillis, Thermal Radiation in Disperse Systems: an Engineering Approach, Begell House, New York, 2010. Online ISBN: 978-1-567000-268-2, Print ISBN: 978-1-567000-268-3.

[30] G.M. Hale, M.P. Querry, Optical constants of water in the 200 nm to 200 μm wavelength region, Appl. Opt. 12 (3) (1973) 555–563, https://doi.org/10.1364/AO.12.000555.
[31] M.P. Querry, W.E. Holland, R.C. Waring, Complex refractive index in the infrared for NaCl, $NaNO_3$, and $NaHCO_3$ in water, J. Opt. Soc. Am. 66 (8) (1976) 830–836, https://doi.org/10.1364/JOSA.66.000830.
[32] D.Q. Chowdhury, P.W. Barber, S.C. Hill, Energy-density distribution inside large nonabsorbing spheres by using Mie theory and geometrical optics, Appl. Opt. 31 (18) (1992) 3518–3523. https://opg.optica.org/ao/abstract.cfm?URI=ao-31-18-3518.
[33] N. Velesco, T. Kaiser, G. Schweiger, Computation of the internal field of a large spherical particle by use of the geometrical-optics approximation, Appl. Opt. 36 (33) (1997) 8724–8728. https://opg.optica.org/ao/abstract.cfm?URI=ao-36-33-8724.
[34] C.J.D. Fell, Y.P. Hutchison, Diffusion coefficients for sodium and potassium chlorides in water at elevated temperatures, J. Chem. Eng. Data 16 (4) (1971) 427–429, https://doi.org/10.1021/je60051a005.
[35] C.H. Hamann, A. Hamnett, W. Vielstich, Electrochemistry, second ed., Wiley-VCH, Weinheim, Germany, 2007. ISBN: 978-3-527-31069-2.
[36] M.E. Perel'man, V.A. Tatarchenko, Phase transitions of the first kind as radiation processes, Phys. Lett. 372 (14) (2008) 2480–2483, https://doi.org/10.1016/j.physleta.2007.11.056.
[37] V.A. Tatarchenko, Characteristic infrared radiation of the first-order phase transitions and its connection with atmospheric optics, Atmos. Ocean. Opt. 23 (4) (2010) 252–258, https://doi.org/10.1134/S1024856010040020.
[38] L.A. Dombrovsky, V.Yu. Levashov, A.P. Kryukov, S. Dembele, J.X. Wen, A comparative analysis of shielding of thermal radiation of fires using mist curtains containing droplets of pure water or sea water, Int. J. Therm. Sci. 152 (2020), 106299, https://doi.org/10.1016/j.ijthermalsci.2020.106299.
[39] A.P. Kryukov, V.Yu. Levashov, I.N. Shishkova, Evaporation in mixture of vapour and gas mixture, Int. J. Heat Mass Tran. 52 (23–24) (2009) 5585–5590.
[40] V.Yu. Levashov, A.P. Kryukov, Numerical simulation of water droplet evaporation into vapor–gas medium, Colloid J. 79 (2017) 647–653, https://doi.org/10.1134/S1061933X1705009X.
[41] D.R. Stull, Vapor pressure of pure substances. Organic and inorganic compounds, Ind. Eng. Chem. 39 (1947) 517–540, https://doi.org/10.1021/ie50448a022.
[42] V.Y. Levashov, A.P. Kryukov, I.N. Shishkova, Influence of the noncondensable component on the characteristics of temperature change and the intensity of water droplet evaporation, Int. J. Heat Mass Tran. 127B (2018) 115–122, https://doi.org/10.1016/j.ijheatmasstransfer.2018.07.069.
[43] V.Yu. Borodulin, V.N. Letushko, M.I. Nizovtsev, A.N. Sterlyagov, Determination of parameters of heat and mass transfer in evaporating drops, Int. J. Heat Mass Tran. 109 (2017) 609–618, https://doi.org/10.1016/j.ijheatmasstransfer.2017.02.042.
[44] A.A. Fedorets, L.A. Dombrovsky, D.N. Gabyshev, E. Bormashenko, M. Nosonovsky, Effect of external electric field on dynamics of levitating water droplets, Int. J. Therm. Sci. 153 (2020), 106375, https://doi.org/10.1016/j.ijthermalsci.2020.106375.
[45] R.G. Cheng, D.C. Blanshard, R.J. Cipriano, The formation of hollow sea-salt particles from the evaporation of drops of sea water, Atmos. Res. 22 (1) (1988) 15–25, https://doi.org/10.1016/0169-8095(88)90009-9.
[46] M. Mezhericher, A. Levi, I. Borde, Theoretical models of single droplet drying kinetics: a review, Drying Tech 28 (2) (2010), https://doi.org/10.1080/07373930903530337.
[47] M.H. Sadafi, I. Jahn, A.B. Stilgoe, Theoretical and experimental studies on a solid containing water droplet, Int. J. Heat Mass Tran. 78 (1) (2014) 25–33, https://doi.org/10.1016/j.ijheatmasstransfer.2014.06.064.
[48] M.H. Sadafi, I. Jahn, A.B. Stilgoe, A theoretical model with experimental verification for heat and mass transfer of saline water, Int. J. Heat Mass Tran. 81 (2015) 1–9, https://doi.org/10.1016/j.ijheatmasstransfer.2014.10.005.
[49] L.A. Dombrovsky, S. Dembele, An improved solution for shielding of thermal radiation of fires using mist curtains of pure water or seawater, Comput. Thermal Sci. 14 (4) (2022) 1–18, https://doi.org/10.1615/ComputThermalScien.2022041314.